Elongational flowinduced microstructure evolutions in polypropylene/layered double hydroxides nanocomposites

INSPIRING PLASTICS PROFESSIONALS

POLYM COMPOSIT

Elongational flow-induced microstructure evolutions in polypropylene/layered double hydroxides nanocomposites

Journal:	*Polymer Composites*
Manuscript ID	PC-23-2957.R4
Wiley - Manuscript type:	Research Article
Date Submitted by the Author:	29-Jan-2024
Complete List of Authors:	Gnoffo, Chiara; Politecnico di Torino Dipartimento Scienza Applicata e Tecnologia Arrigo, Rossella; Politecnico di Torino Dipartimento Scienza Applicata e Tecnologia, Sisani, Michele; Prolabin & Tefarm Srl, Prolabin & Tefarm S.r.l Frache, Alberto; Politecnico di Torino Dipartimento Scienza Applicata e Tecnologia
Keywords:	nanocomposites, mechanical properties, fibers

Editorial Changes REQUIRED:
(a) A graphical abstract of 4.5-inch by 3-inch size and 600 dpi resolution is required. Do not include descriptive text. Need to be a concept figure, not a pile of equipment and data figures with descriptions. Current version does not meet the requirements.
R.) A new version of the graphical abstract complying with the editorial requirements has been prepared and submitted

Referee(s)' Comments to Author:

Reviewing: 1

Comments to the Author
Dear Authors,

I would like to express my appreciation for taking my feedback into account and revising your work. Based on the improvements you have made, I am pleased to recommend the publication of your article in its current form.

Thank you for your hard work and dedication to this project.
R.) We thank the Reviewer for her/his positive evaluation.

Elongational flow-induced microstructure evolutions in polypropylene/layered double hydroxides nanocomposites

Chiara Gnoffo[1], Rossella Arrigo[1,2,*], Michele Sisani[3], Alberto Frache[1,2]

[1] Dipartimento di Scienza Applicata e Tecnologia, Politecnico di Torino, Viale Teresa Michel 5, 15121, Alessandria, Italy

[2] Local INSTM unit

[3] Prolabin & Tefarm S.r.l., Via Dell'Acciaio, 9 06134, Perugia, Italy

Corresponding author: rossella.arrigo@polito.it

Abstract

In this work, the effect of the non-isothermal elongational flow on the morphology and mechanical properties of polypropylene (PP)-based nanocomposites containing Mg-Al layered double hydroxides (LDHs) modified with stearate or oleate functional groups has been investigated. In particular, nanocomposites containing 5 and 10 wt% of LDHs prepared through melt compounding were subjected to uniaxial elongational flow at the exit of the extruder, leading to the formation of fibers characterized by different draw ratios. The mechanical characterization of the fibers demonstrated a progressive enhancement of the tensile strength as a function of the draw ratio with increasing the content of nanofillers. Notably, for the fibers stretched at a draw ratio of 200 and containing 10 wt% of LDHs modified with oleate groups, the tensile strength increased four-fold as compared to that of the unfilled matrix. These results have been attributed to a progressive enhancement of the extent of the dispersions of the embedded LDHs induced by the application of the elongational flow, as also confirmed by morphological analyses. In all, the obtained results demonstrated the beneficial effect of the elongational flow in promoting the achievement of superior mechanical properties in LDHs-containing nanocomposites, hence widening the application field of these nanostructured materials.

Keywords: polypropylene; layered double hydroxides; elongational flow; nanocomposite fibers; mechanical properties.

Highlights

- PP/organomodified LDHs nanocomposites were obtained through melt compounding
- Non-isothermal elongational flow was applied to the extrudates at the die exit
- Anisotropic fibers showed progressively enhanced tensile strength values
- Elongational flow promoted a gradual evolution of the material microstructure
- A gradual improvement of the nanofiller dispersion was observed upon elongation

1. Introduction

Polymer-based nanocomposites have become increasingly popular in the last decades owing to their several advantages in terms of weight, costs and entailing mechanical reinforcement as compared to traditional composites [1–4]. As extensively reported in the literature [5–8], these systems are characterised by sub-micrometric fillers capable of reinforcing the polymeric matrix, due to the nanometric size and the very high surface area of the embedded nanoparticles. In particular, if a good dispersion of the nanoparticles is reached, an extended and complex interface between the nanofillers and the polymer macromolecules is generated, allowing emphasizing the interactions between the two components. Among the nanofillers typically exploited for the formulation of polymer nanocomposites, layered nanoparticles, such as nanoclays and layered double hydroxides (LDHs), can lead to the formation of phase-separated, intercalated or exfoliated structure depending on the dominant interfacial interactions [9]. In particular, when the polymer chains are not able to enter in the space in-between the nanoplatelets, phase-separated composites are achieved, showing properties similar to those of traditional composites [10]. On the other hand, when intercalation occurs, the polymer macromolecules diffuse in the interlayer galleries, usually promoting the obtainment of superior properties [11]. Finally, exfoliated structures are achieved when layered nanoparticles are completely delaminated. In this last case, the polymer/filler interactions are maximized, resulting in the achievement of outstanding final performances [12].

The literature on polymer-based nanocomposites containing layered nanofillers is wide, since this strategy of modification of polymeric materials allows the obtainment of superior properties, while keeping very low the content of solid particles, hence avoiding the increase of the material density caused by the introduction of high contents of mineral fillers typically encountered in conventional composites [13–15]. Nevertheless, most of the literature on this topic concerns polymer nanocomposites containing cationic clays, while less attention has been paid to systems loaded with LDHs, which are very promising materials in several applications [16,17]. In this context, Shi et al. [18] demonstrated that high degrees of exfoliation were achieved in polypropylene (PP)-based nanocomposites containing Mg-Al LDHs modified with dodecylsulfonate/itaconic acid. The formulated nanocomposites exhibited increased crystallinity as compared to the neat matrix, as well as enhanced thermal stability and improved flame-retardant properties. Similarly, Constantino et al. [19-21] demonstrated the beneficial effect of organically modified ZnAl LDHs in improving the thermal stability and fire performance of different polymeric matrices, such as polyethylene and an epoxy resin. Furthermore, from a general point of view, an improvement of the matrix mechanical properties has been reported owing to the introduction of well dispersed LDHs [22].

Several works reported also interesting results for PP-based nanocomposites containing LDHs [23–25]. In this context, when organomodified LDHs are introduced within PP, a general improvement of the thermal stability, crystallinity and mechanical characteristics is documented [26,27]. In particular, it has been shown that well-dispersed LDHs platelets are able to promote heterogeneous nucleation phenomena [28], leading to the achievement of higher melting and recrystallization temperatures as compared to the unfilled matrix [29]. Furthermore, Kakati et al. [24] demonstrated the enhancement of mechanical properties and thermal stability in PP/Ni-Al LDH nanocomposites, leading to better performance of the nanocomposites owing to nanosheets dispersion.

However, one of the main issues concerning the processing of polymer-based nanocomposites is the formation of filler aggregates and agglomerates causing the achievement of uneven and inhomogeneous morphologies, negatively affecting the final properties of the material [25,30]. For this reason, the use of a compatibilizer is mandatory for enhancing the compatibility between the non-polar matrix and the nanofillers, hence allowing obtaining highly intercalated or exfoliated morphologies [31–33].

As documented in the literature, an interesting strategy to enhance the dispersion of the embedded nanofillers in polymer-based nanocomposites involves the application of the elongational flow in non-isothermal conditions. In fact, it has been demonstrated that the applied elongational stresses are effective in inducing a progressive disruption of the filler aggregates and agglomerates typically observed in nanocomposites obtained by melt compounding [34–38], promoting an overall improvement of the material morphology and, hence, final properties. Besides, in the case of polymer nanocomposites containing anisotropic fillers, the applied elongational flow also causes preferential orientation of the embedded nanofillers along the flow direction, inducing superior properties for the systems subjected to stretching as compared to those of their isotropic counterparts [39]. Interestingly, for nanocomposites containing layered fillers, such as nanoclays, a peculiar behavior, involving a sort of elongational flow-induced transition from intercalated to exfoliated morphology, has been reported [40,41]. At present, to the best of the Author's knowledge, most of the investigations in this field concerns polymer-based nanocomposites filled with graphene [42] or nanoclays [43–45]. At variance, only few studies report the formulation of fibres based on nanocomposites containing LDHs through melt spinning [46,47], although the possible elongational flow-induced microstructural evolution on such kind of nanostructured systems has not been systematically elucidated yet.

In this work, the effects of the non-isothermal elongational flow on PP-based nanocomposites containing 5 or 10 wt.% of organomodified was investigated. In particular, two different kinds of nanoparticles, containing two different organomodifiers were introduced within PP through melt compounding. After the characterization of the rheological behavior, thermal properties and

morphology of the isotropic materials, the effect of the non-isothermal elongational flow on the nanocomposite microstructure and mechanical properties was assessed and discussed.

2 Materials and methods

2.1 Materials

PP Moplen HP500N (Melt Flow Rate 12 g/10 min, Density 0.9 g/cm^3, Flexural modulus 1480 MPa from supplier data sheet) supplied by LyondellBasell was chosen as nanocomposites matrix. In order to enhance the LDHs dispersion and the polymer/filler compatibility, maleic anhydride grafted polypropylene (PP-g-MA) from Sigma-Aldrich, with a content of 0.6 wt% of MA was used as compatibilizer. LDHs modified with stearate groups (s-LDHs, $[Mg_{0.66}Al_{0.34}(OH)_2](C_{18}H_{35}O_2)_{0.34}$ x H_2O, D_{50}=1.78 µm, D_{90}=7.60 µm) [48] or with oleate groups (o-LDHs, $[Mg_{0.66}Al_{0.34}(OH)_2](C_{18}H_{33}O_2)_{0.34}$ x H_2O, D_{50}=3.78 µm, D_{90}=10.83 µm) [49] were synthesised by Prolabin&Tefarm.

2.2 Nanocomposites preparation

In order to obtain the nanocomposites, Process 11 Thermo Fisher co-rotating twin screw extruder has been used. The feeder capacity has been set to 100 g/h, while powder feeder to 6 g/h and 12 g/h, so as to obtain nanocomposites containing 5 and 10 wt% of LDHs. The extruder and die temperatures have been set equal to 175°C and 190°C respectively, while the screws rotation has been set equal to 50 rpm.

The materials obtained through melt compounding were then subjected to non-isothermal elongational flow using an IdeaInstr (Italy) RheoSpin apparatus. This equipment allows applying a uniaxial elongational flow to the molten extrudate coming out from the extruder through a series of pulleys which catch the hot filament and convey it to a final pulley rotating at steady speed or acceleration. Since the uniaxial stretching occurs at room temperature, the filament cools down gradually during the elongation, until solidification. In this way, fibers at different draw ratio ($DR = diameter^2_{extrudate}/diameter^2_{fiber}$) can be prepared and collected.

2.3 Characterization techniques

Bruker D2 Phaser 2nd generation X-ray Powder Diffractometer equipped with LYNXEYE SSD160 detector has been used to analyse pristine PP and nanocomposites. The apparatus has a CuKα radiation operating at 30 kV and 15 mA. The step size (2θ) was 0.1° from 1.5 up to 40° and time per step was equal to 0.2 s. Both pristine LDHs and extruded nanocomposites were characterized. Specimens for XRD characterization were obtained through a compression molding step, using a laboratory press Collin P 200 T at 190°C.

Rheological analysis has been conducted via ARES TA Instruments parallel plate rheometer with a plate diameter equal to 25 mm. Preliminary strain sweep tests (to evaluate the linear viscoelastic range of the materials) and frequency sweep measurements were performed at 190°C, equivalent to the processing temperature. The former was characterized by a frequency equal to 10 rad/s, with strain values between 0.1 and 300%, while during the latter, frequency values ranged from 100 rad/s to 0.1 rad/s for pristine PP and to 0.01 rad/s for nanocomposites. The samples, with diameter equal to 25 mm and thickness equal to 1 mm, were obtained using a laboratory press Collin P 200 T at 190°C. After a 3-minute pre-heating, the pellets were pressed for 2 minutes at 100 bar into a metallic mould. For thermal characterization, TA Instruments DSC Q20 has been used with the following thermal cycle (performed under nitrogen atmosphere): a first heating scan from -50°C to 200°C, isothermal step at 200 °C for 3 minutes, a cooling scan from 200 to -50 °C and a second heating ramp from -50°C to 200°C. During all the steps, the rate of heating/cooling was maintained at 10 °C/min. The crystallinity content of the samples was calculated through the following formula [50]:

$$\chi_C = 100 * \frac{\Delta H_M}{\Delta H_{M100\%} * (1 - x)} \quad (2)$$

where ΔH_M is the melting enthalpy (evaluated as the area of the melting peak recorded during the second heating scan), $\Delta H_{M100\%}$ is the melting enthalpy of the 100% crystalline PP (207 J/g [51]) and x is the nanofiller content.

For morphological characterization, Zeiss LEO-1450PV SEM has been used on fracture surfaces with a sputtered fold layer of both extrudates and fibers. In order to obtain brittle fracture, the sample have been treated in liquid nitrogen for several minutes before fracturing.

Mechanical characterization of the fibers was performed using an Instron 5966 dynamometer at room temperature equipped with a 2 kN load cell, at a crosshead speed of 100 mm/min.

3 Results and discussion

3.1 Characterization of the nanocomposites extrudates (isotropic samples)

Figures 1a and 2a show the trends of the complex viscosity (η*) for the nanocomposites containing s-LDHs or o-LDHs, respectively. Unfilled PP shows the typical Newtonian behavior in the low frequency region, followed by a mild shear thinning at high frequencies. Differently, the introduction of LDHs, irrespective of the type of the organomodifier, involves a substantial variation of this behavior. In fact, the rheological response of the LDHs-containing systems shows remarkable non-Newtonian features, involving the amplification of the shear thinning at high frequencies and the appearance of a yield stress behavior in the low frequency region, which is more pronounced for the systems containing higher loadings of LDHs. The observed modification of the PP rheological behavior resulting from the introduction of the nanofillers can be ascribed to the establishment of

strong interactions between the high-aspect-ratio LDHs particles and the PP chains, which hamper the relaxation dynamics of the polymer macromolecules [8,52]. Besides, as already demonstrated for similar nanocomposites containing modified LDHs [53], the effect of the embedded nanoparticles on the matrix rheological behavior could be also attributed to the restrained mobility of the macromolecular chains, due to the partial immobilization of the macromolecules on the LDH surface or in between the platelets (in the case of intercalated structures). Finally, the slight lower complex viscosity of the nanocomposites as compared to unfilled PP in the high frequency region can be associated with the preferential alignment of the embedded nanofillers along the flow direction [23,33,54].

Looking at the trends of the storage modulus (G') reported in Figure 1b and 2b, for the nanocomposites a gradual flattening of the curves at low frequencies can be observed, with the achievement of a sort of plateau which is more distinct with increasing the LDHs loading. According to the literature and to what inferred before from the analysis of the complex viscosity curves, this feature can be explained considering the slowdown of the relaxation dynamics of the polymer chains induced by the presence of well dispersed embedded nanofillers, causing a transition from liquid-like to solid-like rheological behavior [55–57].

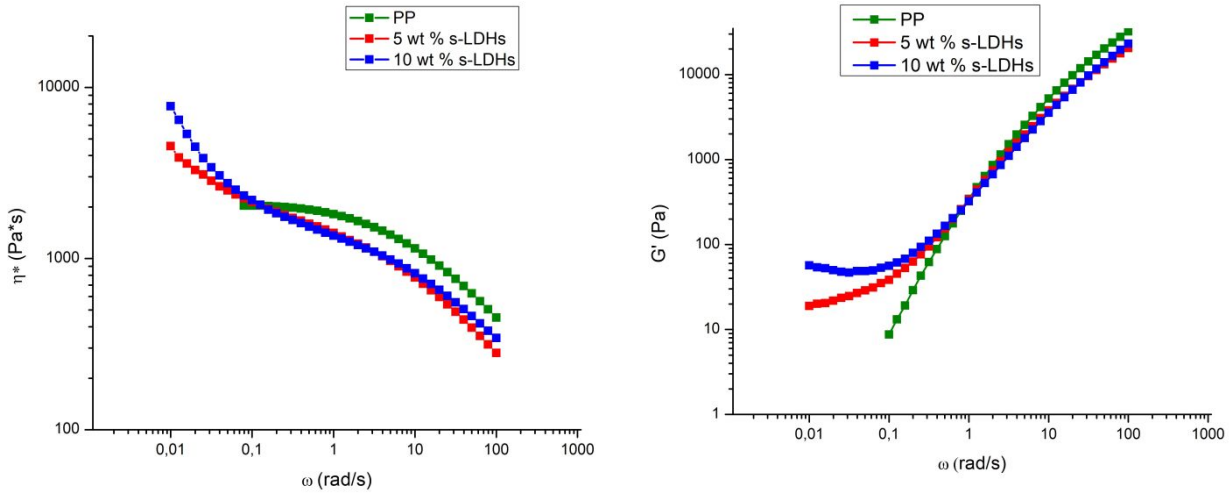

(a) **(b)**

Figure 1. Complex viscosity η* (a) and storage modulus G' (b) as a function of frequency for extruded PP/s-LDHs nanocomposites

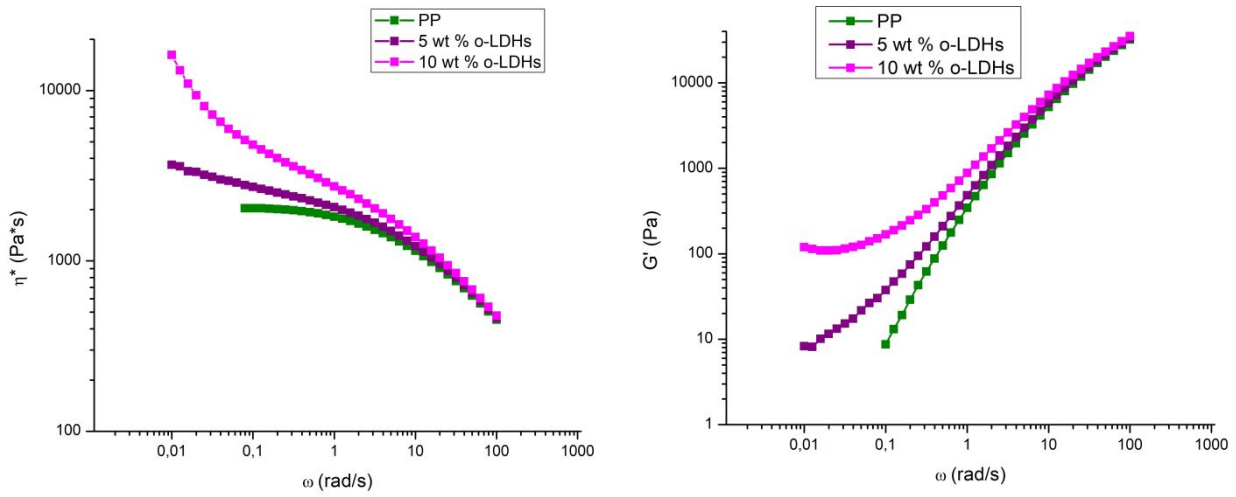

(a) **(b)**

Figure 2. Complex viscosity η* (a) and storage modulus G' (b) as a function of frequency for extruded PP/o-LDHs nanocomposites

Aiming at evaluating the morphology of the nanocomposites achieved through the melt compounding and at assessing the possible formation of intercalated or partially exfoliated structures, XRD analyses were carried out. Figure 3 shows the diffractograms for unfilled PP, organomodified LDHs and all formulated nanocomposites in the region in which lie the typical signals of LDHs. According to the literature [58], the diffractograms of the organomodified LDHs indicate that the particles have crystalline nature and layered geometry, with two main peaks corresponding to the 003 (basal peak) and 006 (higher order reflection) crystallographic planes, centered at 2.5° and 5.6°, respectively, regardless the kind of organomodifier group. For the nanocomposites, the introduction of the nanofillers does not result in significant modifications of the matrix crystallographic structure [59]. Furthermore, for the systems containing low content of organomodified nanoparticles (i.e. 5 wt %) the LDHs peaks disappeared. This result can be attributed either to the achievement of highly intercalated/exfoliated morphologies or to the low loading of nanofillers, which makes insensitive the XRD analysis [60]. At variance, for the nanocomposites containing 10 wt % of nanofillers some differences can be noticed. Firstly, for the system containing s-LDHs weak signals attributable to both basal and higher order reflection peaks can be observed, suggesting that the embedded particles are mainly dispersed as separated platelets, giving rise to the formation of intercalated or exfoliated structures. On the other hand, the basal peak is remarkably evident in the diffractogram of the nanocomposite containing 10 wt% of o-LDHs, indicating in this case the presence of some stacked LDHs structures (i.e. tactoids) embedded in the polymer matrix.

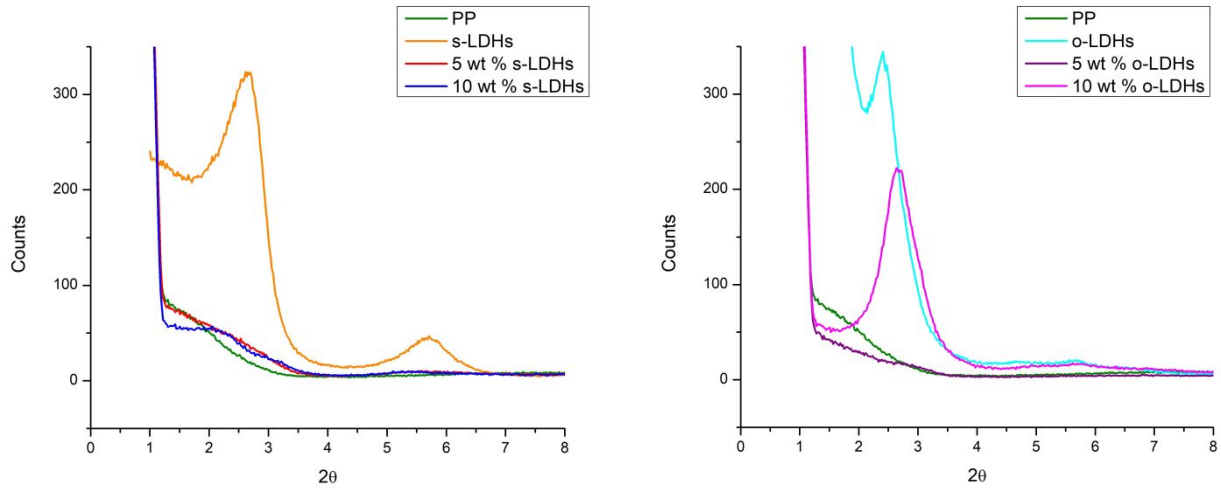

(a) **(b)**

Figure 3. XRD diffractograms for s-LDHs and s-LDHs nanocomposites (a) and o-LDHs and o-LDHs nanocomposites (b). The diffractogram of unfilled PP is also reported.

To gain further insights into the morphology of the formulated nanocomposites, SEM characterization was carried out. The micrographs reported in Figure 4, referring to the systems containing the highest amount of both kinds of organomodified LDHs, highlight the achievement of an uneven dispersion of the embedded nanofillers, confirming the results coming from XRD analyses. In particular, for both nanocomposites it is possible to observe portions in which the nanofillers are well dispersed and distributed at sub-micrometric scale, notwithstanding the presence of aggregates having micrometric dimensions. Actually, also the performed EDX analyses (reported in Figure S1) indicate that the nanofillers are homogeneously visible on the whole investigated surfaces, without portions in which the LDHs are not present. Therefore, it can be inferred that most of the introduced LDHs are effectively able to form intercalated or exfoliated hybrids, although a portion of them remains in the stacked form, with occasional clustering and agglomeration. In all, the performed XRD and morphological characterizations indicate that the melt compounding step was not fully effective in promoting the achievement of large degrees of intercalation or exfoliation. In fact, it can be inferred that the embedded nanofillers are largely dispersed as thin platelets, giving rise to intercalation/exfoliation phenomena, although the presence of some agglomerates involving stacked tactoids. As a matter of fact, as widely reported in the literature [61], differently from conventional cationic nanoclays, the hydroxide platelets are characterized by very high values of surface charge density, which make very difficult the obtainment of consistent levels of exfoliation.

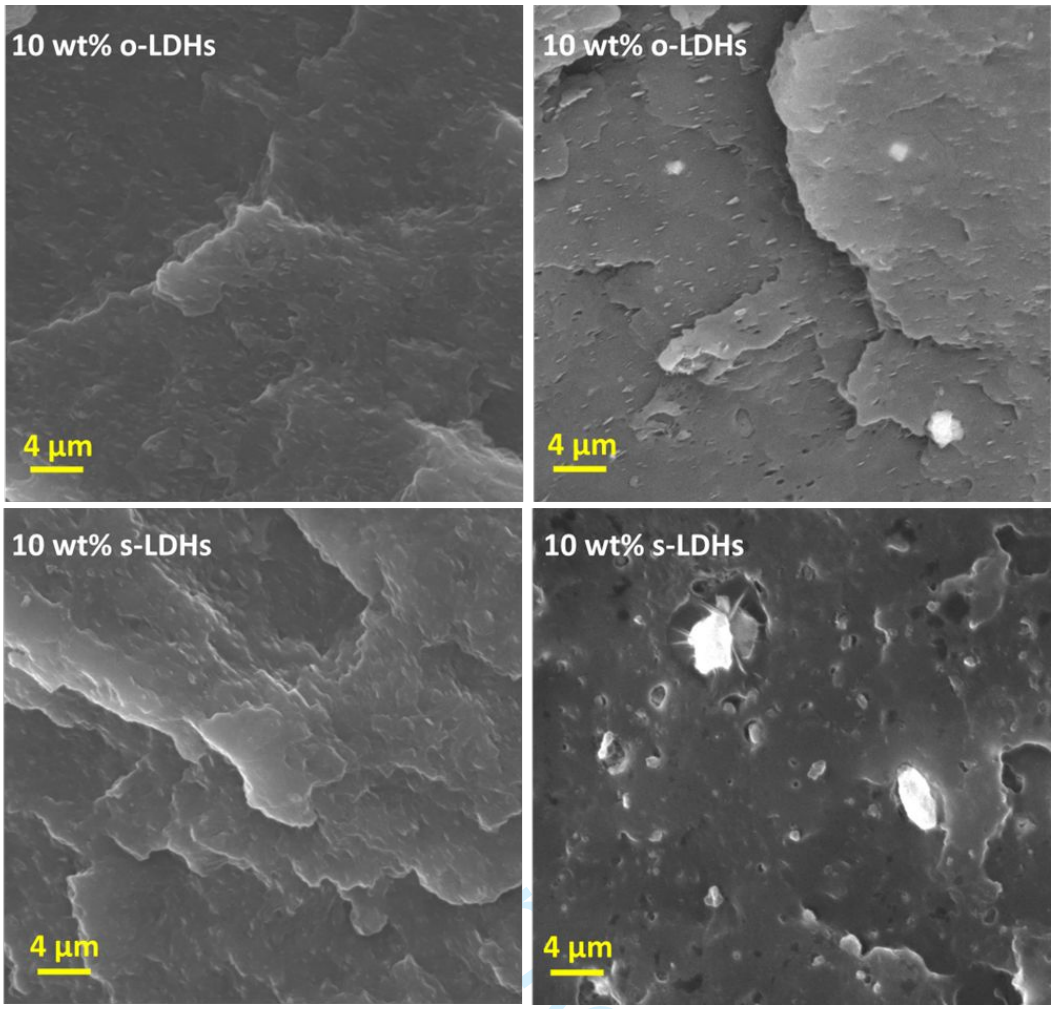

Figure 4. SEM micrographs of isotropic (melt compounded) nanocomposites containing 10 wt % of o-LDHs or s-LDHs.

Figures 5 a and b report the thermograms recorded during the cooling and the second heating scans, respectively, for unfilled PP and all formulated nanocomposites. The main thermal properties (i.e., melting enthalpy ΔH_M and crystallinity degree χ) collected during the second heating ramp are listed in Table 1**Error! Reference source not found.**. The introduction of LDHs induced an anticipation of the crystallization, as well as an increase in the crystallinity content, indicating a nucleating effect exerted by the embedded nanofillers [59,62–65]. Furthermore, it can be observed that LDHs-containing nanocomposites, unlike to the unfilled PP, show two melting peaks, with a secondary event at 150 °C. According to the literature, the peak at lower temperature can be likely associated with the melting of smallest crystallites that are formed through secondary crystallization processes in the inter-lamellar space between the larger crystallites [66].

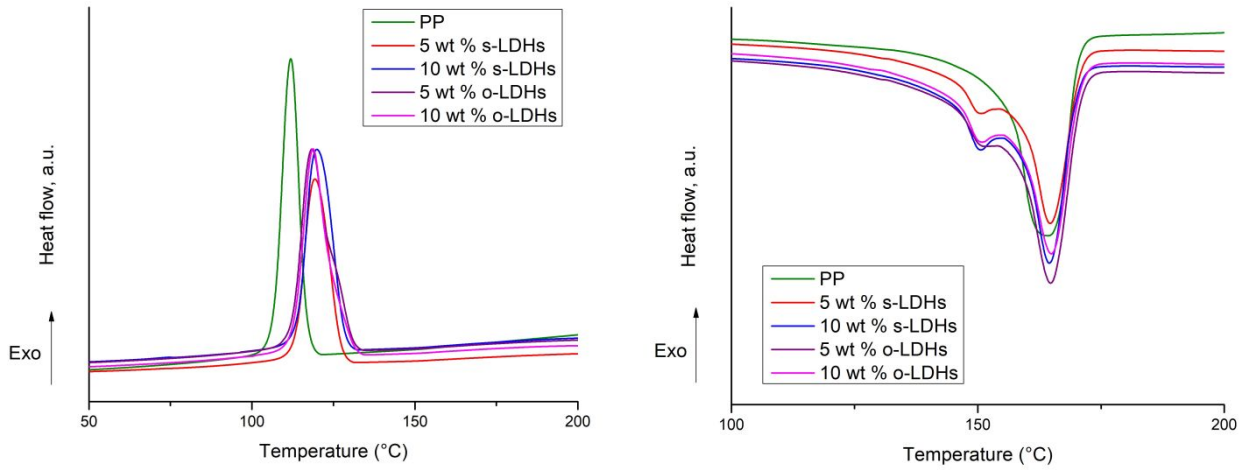

Figure 5. DSC thermograms for all investigated systems recorded during the cooling (a) and the second heating (b) scans.

	ΔH_M [J/g]	χ [%]
PP	86.7	42%
5 wt % s-LDHs	73.5	36%
10 wt % s-LDHs	87.7	42%
5 wt % o-LDHs	96.6	47%
10 wt % o-LDHs	89.4	43%

Table 1. Melting enthalpy (ΔH_M) and crystallinity degree (χ) evaluated during the second heating scan for unfilled PP and all LDHs-containing nanocomposites.

3.2 Characterization of nanocomposites fibers (anisotropic samples)

Aiming at assessing the possible effect of the application of the non-isothermal elongational flow on the morphology and, hence, on the mechanical properties of the LDHs-containing nanocomposites, the fibers at different draw ratios (obtained by subjecting the molten extrudates to a uniaxial stretching, as already described in paragraph 2.2) were characterized through tensile tests. The obtained results, in terms of variation of the dimensionless tensile strength as a function of DR, are depicted in Figures 6 (a-b). The dimensionless values were obtained as the ratio between the measured values of the tensile strength of the fiber at a given DR and the value of the tensile strength of the corresponding isotropic sample (reported in Table S1). This representation of the data allows for emphasizing the effect of the elongational flow and thus of the orientation phenomena, regardless the intrinsic mechanical characteristics of the starting isotropic material [67]. As far as the unfilled PP is

concerned, an almost linear increase of the tensile strength as a function of DR can be observed. This behavior can be ascribed to the well-known effect of the elongational flow in inducing a preferential orientation of the polymer macromolecules along the flow direction [68]. For the nanocomposites containing 5 wt% of both kinds of organomodified LDHs, a trend very similar to that of the neat PP can be recognised. More specifically, for the system containing s-LDHs the obtained data tend to superimpose those of unfilled matrix, indicating that the introduction of the nanofillers did not significantly affect the tensile behavior of the PP fibers. Differently, the introduction of 5 wt% of o-LDHs brings about an increase of the tensile strength for all tested DR, and the fibers at DR=400 show a quadrupled tensile strength as compared to that of the unfilled PP. However, the slope of the trend of tensile strength as a function of DR is almost unchanged as compared to that of the unfilled matrix. This last indicates that the observed increase of the tensile properties can be solely ascribed to the progressive orientation of the PP chains. On the other hand, the nanocomposites containing higher loadings of nanofillers show a very different behavior. In particular, these systems exhibit higher values of tensile strength, with respect to either neat PP or systems containing a lesser amount of LDHs, especially at high DR. In fact, for the materials stretched at DR = 200, the tensile strength reached values which are three-fold and four-fold higher than those of neat PP, when s-LDHs and o-LDHs, respectively, are introduced within the polymeric matrix. This feature suggests that, upon the application of the elongational flow, beside the progressive orientation of the polymer chains along the stretching direction (causing a gradual reinforcing effect), some other phenomena promoting a gradual enhancement of the tensile strength of the nanocomposite fibers occur. According to the literature [42,69], this further reinforcing mechanism can be attributed to a progressive evolution of the material morphology resulting from the application of the elongation. More specifically, it can be inferred that the applied elongational flow has a beneficial effect on the extent of dispersion and distribution of the nanofillers, inducing a partial disruption of the aggregates of LDHs which are still present at the end of the melt compounding step (as testified by the SEM and XRD characterizations discussed before).

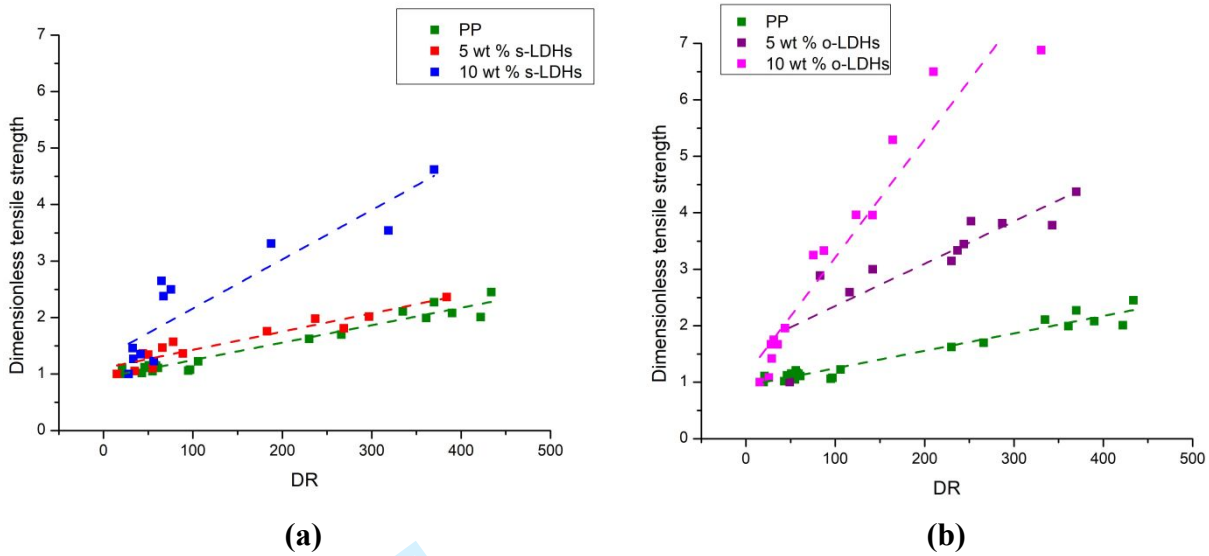

(a) **(b)**

Figure 6. Dimensionless tensile strength as a function of draw ratio (DR) for s-LDHs- (a) and o-LDHs-containing nanocomposite fibers. Data for unfilled PP are also reported.

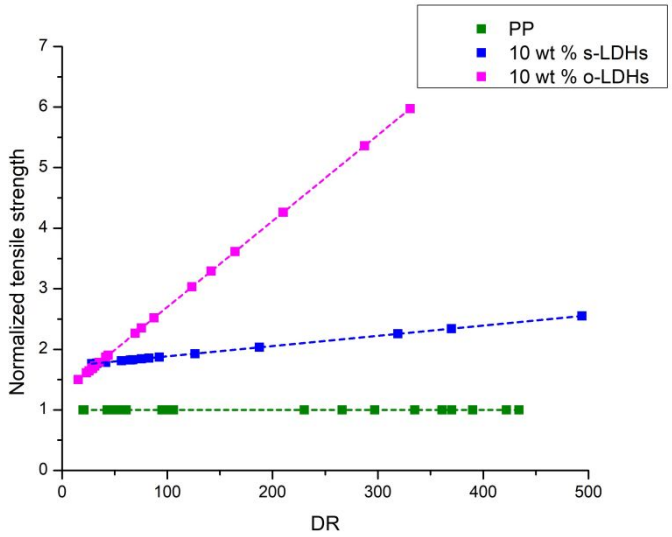

Figure 7. Normalized tensile strength as a function of draw ratio (DR) for unfilled PP and nanocomposites fibers containing 10 wt% of s-LDHs or o-LDHs.

To gain further insights into the inferred phenomena occurring during the application of the elongational flow, the dimensionless tensile strength values for the nanocomposites containing 10 wt% of both types of organomodified LDHs were normalized with respect to the dimensionless values of unfilled PP. The obtained results are plotted in Figure 7 as a function of the draw ratio. This procedure allows removing the reinforcing effect due to the orientation phenomena involving the polymer chains, highlighting even more the influence of the embedded nanofillers and the possible evolution of their dispersion upon stretching. In other words, the achievement of a flat line indicates that the observed growth of the tensile strength as a function of DR can be solely attributed to the

orientation of the polymer chains induced by the uniaxial elongation. At variance, a trend with a higher slope would demonstrate the occurrence of some evolution of the material morphology, mainly involving the nanofillers. As observable in Figure 7, for the system containing s-LDHs a trend very similar to that of unfilled PP is obtained. This feature indicates that, in this case, the predominant reinforcing mechanism is associated with the orientation of the PP chains along the flow direction. Differently, in the case of the fibers containing o-LDHs, a remarkable increase of the tensile strength is observed, demonstrating that the material morphology is able to evolve and modify upon the application of the elongational flow. As anticipated before, this evolution concerns a progressive disruption of the nanofiller clusters observed after the melt compounding step. Additionally, it is possible to infer that, similarly to what reported in the literature for fibers containing anionic nanoclays, the application of the elongational flow also induces an increase of the interlayer distance either in the tactoids or in the intercalated hybrids already present in the melt-compounded nanocomposites, bringing about to an amplification of the intercalation phenomena or, possibly, to the formation exfoliated structures [41]. Furthermore, a preferential orientation of the embedded nanofillers along the flow direction, further contributing to enhance the tensile strength of the fibers, can not be excluded [43]. Looking at the differences observed between the fibers containing s-LDHs or o-LDHs, it should be considered that, during the application of the elongational flow, the progressive enhancement of the state of dispersion of the embedded nanofillers (and also the possible increase of the interlayer distance promoting the formation of intercalated/exfoliated hybrids) is in competition with flocculation phenomena. These lasts can cause the formation of nanofiller clusters due to the decreased distance between the embedded nanofillers induced by the stretching [70,71]. As widely documented in the literature, the flocculation is prevalent when the elongational flow is applied in isothermal conditions (since the low viscosity of the matrix allows the re-arrangement of the dispersed particles) or in systems which are already characterized by high degrees of intercalation/exfoliation before the application of the stretching [41,72]. As far as the systems object of this work are concerned, XRD analyses demonstrated the formation of intercalated/exfoliated structures in the isotropic (melt compounded) nanocomposite with embedded 10 wt% of s-LDHs, while the system containing the same loading of o-LDHs exhibited a well-developed basal peak attributed to the presence of stacked tactoids. Therefore, it is possible to infer that the application of the elongational flow was less effective in inducing microstructural evolution in the nanocomposite for which a better degree of nanofiller dispersion and distribution was achieved during the melt compounding step.

The morphological characterization performed through SEM observations confirms what inferred on the basis of the analysis of the fiber tensile behavior. In fact, as observable in Figure 8, for the fibers

containing 10 wt% of s-LDHs the presence of some nanofiller cluster, likely resulting from the aforementioned flocculation phenomena promoted by the application of the elongational flow, can be observed. Otherwise, the anisotropic samples with embedded the same amount of o-LDHs show a homogeneous morphology, and no nanofiller aggregates can be observed at the exploited magnification. This result clearly demonstrates the beneficial effect of the elongational flow in inducing some evolutions of the nanocomposite morphology leading to the achievement of higher degree of intercalation and/or exfoliation.

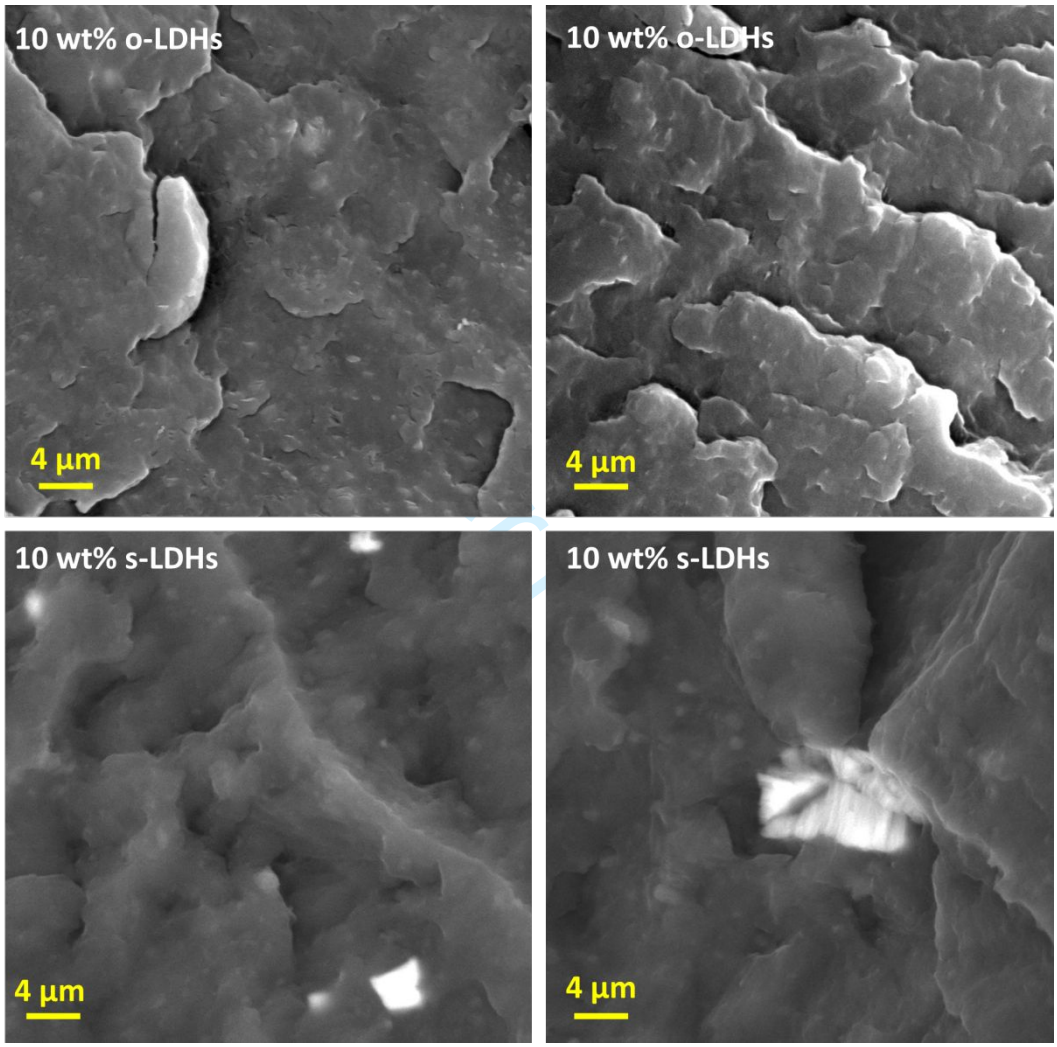

Figure 8. SEM micrographs of nanocomposite fibers at DR 300 containing 10 wt % of o-LDHs or s-LDHs.

4. Conclusion

In this work, PP-based nanocomposites loaded with 5 or 10 wt % of Mg-Al LDHs modified with stearate or oleate functional groups have been investigated, with particular attention to the effect of elongational flow on the morphology and, hence, mechanical properties of the formulated materials. The obtained results demonstrated that the melt compounding step, performed through a twin-screw extruder, was not fully effective for the obtainment of a homogeneous morphology. In fact, although

the performed rheological analyses indicated the achievement of strong polymer/filler interactions strongly affecting the relaxation dynamics of the matrix macromolecules, XRD and SEM characterization testified the presence of some nanofiller clusters (having micrometric dimensions), associable with the presence of stacked tactoids, especially for the nanocomposite containing o-LDHs. The application of a non-isothermal elongational flow to the isotropic nanocomposite resulted in the achievement of a progressively higher tensile strength as a function of draw ratio, especially for the systems containing 10 wt% of both kinds of LDHs. In particular, the fibers stretched at DR of 200, containing s-LDHs and o-LDHs showed values of tensile strength tripled and quadrupled, respectively, as compared to those of unfilled PP. The obtained results were ascribed to the progressive disruption of the nanofiller aggregates still present after the melt compounding step, induced by the application of the uniaxial stretching. Furthermore, for the fibers containing 10 wt% of o-LDHs a further reinforcing mechanism induced by the application of the elongational flow was proposed. In particular, it was inferred that, similarly to traditional nanoclays-containing nanocomposites, the application of the elongational flow can promote a gradual evolution of the system morphology, involving a progressive increase of the distance between the LDH platelets that caused the achievement of a higher intercalation (or exfoliation) level as compared to the isotropic systems. In all, the obtained results could help in opening new perspectives on the exploitation of LDHs-containing nanocomposites in some industrially relevant application fields, such as packaging, in which the produced items are typically subjected to non-isothermal elongational flow during the productive process.

References

[1] S. Fu, Z. Sun, P. Huang, Y. Li, N. Hu. Some basic aspects of polymer nanocomposites: A critical review, Nano Materials Science. 1 (2019) 2-30. https://doi.org/ 10.1016/j.nanoms.2019.02.006.

[2] J. Jordan, K.I. Jacob, R. Tannenbaum, M.A. Sharaf, I. Jasiuk. Experimental trends in polymer nanocomposites—a review, Materials Science and Engineering: A. 393 (2005) 1-11. https://doi.org/10.1016/j.msea.2004.09.044

[3] Q.H. Zeng, A.B. Yu, G.Q. Lu. Multiscale modeling and simulation of polymer nanocomposites, Progress in Polymer Science. 33 (2008) 191-269. https://doi.org/10.1016/j.progpolymsci.2007.09.002.

[4] J. Zhao, L. Wu, C. Zhan, Q. Shao, Z. Guo, L. Zhang. Overview of polymer nanocomposites: Computer simulation understanding of physical properties, Polymer. 133 (2017) 272-287. https://doi.org/10.1016/j.polymer.2017.10.035.

[5] H. Fischer, Polymer nanocomposites: From fundamental research to specific applications, Materials Science and Engineering C. 23 (2003) 763–772. https://doi.org/10.1016/j.msec.2003.09.148.

[6] S. Pavlidou, C.D. Papaspyrides, A review on polymer-layered silicate nanocomposites, Progress in Polymer Science (Oxford). 33 (2008) 1119–1198. https://doi.org/10.1016/j.progpolymsci.2008.07.008.

[7] D.R. Paul, L.M. Robeson, Polymer nanotechnology: Nanocomposites, Polymer. 49 (2008) 3187–3204. https://doi.org/10.1016/j.polymer.2008.04.017.

[8] R. Krishnamoorti, K. Yurekli, Rheology of polymer layered silicate nanocomposites, Current Opinion in Colloid & Interface Science. 6 (2001) 464-470. https://doi.org/10.1016/S1359-0294(01)00121-2.

[9] M. Alexandre, P. Dubois, Polymer-layered silicate nanocomposites: preparation, properties and uses of a new class of materials, Mater. Sci. Eng. R Rep. 28 (2000) 1-63. https://doi.org/10.1016/S0927-796X(00)00012-7.

[10] M. Zanetti, S. Lomakin, G. Camino, Polymer layered silicate nanocomposites, Macromol Mater Eng. 279 (2000) 1–9. https://doi.org/10.1002/1439-2054(20000601)279:1<1::AID-MAME1>3.0.CO;2-Q.

[11] C.W. Chiu, T.K. Huang, Y.C. Wang, B.G. Alamani, J.J. Lin, Intercalation strategies in clay/polymer hybrids, Prog Polym Sci. 39 (2014) 443–485. https://doi.org/10.1016/j.progpolymsci.2013.07.002.

[12] T.T. Zhu, C.H. Zhou, F.B. Kabwe, Q.Q. Wu, C.S. Li, J.R. Zhang, Exfoliation of montmorillonite and related properties of clay/polymer nanocomposites, Appl Clay Sci. 169 (2019) 48–66. https://doi.org/10.1016/j.clay.2018.12.006.

[13] T.S. Ellis, J.S. D'Angelo, Thermal and mechanical properties of a polypropylene nanocomposite, J Appl Polym Sci. 90 (2003) 1639–1647. https://doi.org/10.1002/app.12830.

[14] M. Kotal, A.K. Bhowmick, Polymer nanocomposites from modified clays: Recent advances and challenges, Prog Polym Sci. 51 (2015) 127–187. https://doi.org/10.1016/j.progpolymsci.2015.10.001.

[15] V. Kumar, A. Singh, Polypropylene clay nanocomposites, Reviews in Chemical Engineering. 29 (2013) 439–448. https://doi.org/10.1515/revce-2013-0014.

[16] J.I. Velasco, M. Ardanuy, M. Antunes, Layered double hydroxides (LDHs) as functional fillers in polymer nanocomposites, in: Advances in Polymer Nanocomposites: Types and Applications, Elsevier Inc., 2012: pp. 91–130. https://doi.org/10.1533/9780857096241.1.91.

[17] F. Leroux, J. Besse, Polymer interleaved layered double hydroxide: A new emerging class of nanocomposites, Chemistry of Materials. 13 (2001) 3507–3515. https://doi.org/10.1021/cm0110268.

[18] Y. Shi, F. Chen, J. Yang, M. Zhong, Crystallinity and thermal stability of LDH/polypropylene nanocomposites, Appl Clay Sci. 50 (2010) 87–91. https://doi.org/10.1016/j.clay.2010.07.007.

[19] U. Costantino, A. Gallipoli, M. Nocchetti, G. Camino, F. Bellucci, A. Frache, New nanocomposites constituted of polyethylene and organically modified ZnAl-hydrotalcites, Polym Degrad Stab. 90 (2005) 586–590. https://doi.org/10.1016/j.polymdegradstab.2005.05.019.

[20] U. Costantino, F. Montanari, M. Nocchetti, F. Canepa, A. Frache, Preparation and characterisation of hydrotalcite/carboxyadamantane intercalation compounds as fillers of polymeric nanocomposites, J Mater Chem. 17 (2007) 1079–1086. https://doi.org/10.1039/b613842j.

[21] A. Frache, O. Monticelli, M. Nocchetti, G. Tartaglione, U. Costantino, Thermal properties of epoxy resin nanocomposites based on hydrotalcites, Polym Degrad Stab. 96 (2011) 164–169. https://doi.org/10.1016/j.polymdegradstab.2010.10.006.

[22] T. Nogueira, R. Botan, F. Wypych, L. Lona, Study of thermal and mechanical properties of PMMA/LDHs nanocomposites obtained by in situ bulk polymerization, Compos Part A Appl Sci Manuf. 42 (2011) 1025–1030. https://doi.org/10.1016/j.compositesa.2011.04.006.

[23] S.P. Lonkar, S. Therias, F. Leroux, J.L. Gardette, R.P. Singh, Thermal, mechanical, and rheological characterization of polypropylene/layered double hydroxide nanocomposites, Polym Eng Sci. 52 (2012) 2006–2014. https://doi.org/10.1002/pen.23147.

[24] K. Kakati, G. Pugazhenthi, P.K. Iyer, Effect of organomodified Ni-Al layered double hydroxide (OLDH) on the properties of polypropylene (PP)/LDH nanocomposites, International Journal of Polymeric Materials and Polymeric Biomaterials. 61 (2012) 931–948. https://doi.org/10.1080/00914037.2011.610060.

[25] S. Naseem, S. Wießner, I. Kühnert, A. Leuteritz, Layered double hydroxide (Mgfeal-ldh)-based polypropylene (pp) nanocomposite: Mechanical properties and thermal degradation, Polymers (Basel). 13 (2021). https://doi.org/10.3390/polym13193452.

[26] B. Nagendra, K. Mohan, E. Bhoje Gowd, Polypropylene/Layered Double Hydroxide (LDH) Nanocomposites: Influence of LDH Particle Size on the Crystallization Behavior of Polypropylene, ACS Appl Mater Interfaces. 7 (2015) 12399–12410. https://doi.org/10.1021/am5075826.

[27] D.Y. Wang, A. Leuteritz, B. Kutlu, M.A. Der Landwehr, D. Jehnichen, U. Wagenknecht, G. Heinrich, Preparation and investigation of the combustion behavior of polypropylene/organomodified MgAl-LDH micro-nanocomposite, J Alloys Compd. 509 (2011) 3497–3501. https://doi.org/10.1016/j.jallcom.2010.12.138.

[28] S.P. Lonkar, R.P. Singh, Isothermal crystallization and melting behavior of polypropylene/layered double hydroxide nanocomposites, Thermochim Acta. 491 (2009) 63–70. https://doi.org/10.1016/j.tca.2009.03.002.

[29] Q. Wang, X. Zhang, C.J. Wang, J. Zhu, Z. Guo, D. O'Hare, Polypropylene/layered double hydroxide nanocomposites, J Mater Chem. 22 (2012) 19113–19121. https://doi.org/10.1039/c2jm33493c.

[30] P. Kiliaris, C.D. Papaspyrides, Polymer/layered silicate (clay) nanocomposites: An overview of flame retardancy, Progress in Polymer Science. 35 (2010) 902–958. https://doi.org/10.1016/j.progpolymsci.2010.03.001.

[31] M.L. López-Quintanilla, S. Sánchez-Valdés, L.F. Ramos De Valle, F.J. Medellín-Rodríguez, Effect of some compatibilizing agents on clay dispersion of polypropylene-clay nanocomposites, J Appl Polym Sci. 100 (2006) 4748–4756. https://doi.org/10.1002/app.23262.

[32] A. Tidjani, O. Wald, M.M. Pohl, M.P. Hentschel, B. Schartel, Polypropylene-graft-maleic anhydride-nanocomposites: I - Characterization and thermal stability of nanocomposites produced under nitrogen and in air, Polym Degrad Stab. 82 (2003) 133–140. https://doi.org/10.1016/S0141-3910(03)00174-5.

[33] S.H. Lee, E.N.R. Cho, J.R. Youn, Rheological behavior of polypropylene/layered silicate nanocomposites prepared by melt compounding in shear and elongational flows, J Appl Polym Sci. 103 (2007) 3506–3515. https://doi.org/10.1002/app.25204.

[34] T. Wu, Y. Tong, F. Qiu, D. Yuan, G. Zhang, J. Qu, Morphology, rheology property, and crystallization behavior of PLLA/OMMT nanocomposites prepared by an innovative eccentric rotor extruder, Polym Adv Technol. 29 (2018) 41–51. https://doi.org/10.1002/pat.4087.

[35] M.A. de Goes, L.A. Woicichowski, R.V.V. da Rosa, J.P.F. Santos, B. de M. Carvalho, Improving the dispersion of MWCNT and MMT in PVDF melts employing controlled extensional flows, J Appl Polym Sci. 138 (2021). https://doi.org/10.1002/app.50274.

[36] T. Wu, Z.X. Huang, D.Z. Wang, J.P. Qu, Effect of continuous elongational flow on structure and properties of short glass fiber reinforced polyamide 6 composites, Advanced Industrial and Engineering Polymer Research. 2 (2019) 93–101. https://doi.org/10.1016/j.aiepr.2019.06.003.

[37] M. Tokihisa, K. Yakemoto, T. Sakai, L.A. Utracki, M. Sepehr, J. Li, Y. Simard, Extensional flow mixer for polymer nanocomposites, in: Polym Eng Sci, 2006: pp. 1040–1050. https://doi.org/10.1002/pen.20542.

[38] Z. Yuan, X. Chen, D. Yu, P. Fernandes, A. Faroughi, L.L. Ferrás, A.M. Afonso, Recent Advances in Elongational Flow Dominated Polymer Processing Technologies, Polymers 13 (2021) 1792. https://doi.org/10.3390/polym.

[39] N.T.Z. Dintcheva, R. Arrigo, M. Morreale, F.P. La Mantia, R. Matassa, E. Caponetti, Effect of elongational flow on morphology and properties of polymer/CNTs nanocomposite fibers, Polym Adv Technol. 22 (2011) 1612–1619. https://doi.org/10.1002/pat.1648.

[40] F.P. La Mantia, R. Arrigo, M. Morreale, Effect of the orientation and rheological behaviour of biodegradable polymer nanocomposites, Eur Polym J. 54 (2014) 11–17. https://doi.org/10.1016/j.eurpolymj.2014.02.007.

[41] F.P. La Mantia, N.T. Dintcheva, R. Scaffaro, R. Marino, Morphology and properties of polyethylene/clay nanocomposite drawn fibers, Macromol Mater Eng. 293 (2008) 83–91. https://doi.org/10.1002/mame.200700204.

[42] F.P. La Mantia, M. Ceraulo, M.C. Mistretta, L. Botta, Effect of the elongational flow on morphology and properties of polypropylene/graphene nanoplatelets nanocomposites, Polym Test. 71 (2018) 10–17. https://doi.org/10.1016/j.polymertesting.2018.08.016.

[43] B. Coppola, P. Scarfato, L. Incarnato, L. Di Maio, Morphology development and mechanical properties variation during cold-drawing of polyethylene-clay nanocomposite fibers, Polymers (Basel). 9 (2017). https://doi.org/10.3390/polym9060235.

[44] A. Bafna, G. Beaucage, F. Mirabella, S. Mehta, 3D Hierarchical orientation in polymer-clay nanocomposite films, Polymer, 44, 4 (2003). https://doi.org/10.1016/S0032-3861(02)00833-9.

[45] R.K. Gupta, V. Pasanovic-Zujo, S.N. Bhattacharya, Shear and extensional rheology of EVA/layered silicate-nanocomposites, J Nonnewton Fluid Mech. 128 (2005) 116–125. https://doi.org/10.1016/j.jnnfm.2005.05.002.

[46] B. Kutlu, J. Meinl, A. Leuteritz, H. Brünig, G. Heinrich, Melt-spinning of LDH/HDPE nanocomposites, Polymer (Guildf). 54 (2013) 5712–5718. https://doi.org/10.1016/j.polymer.2013.08.015.

[47] B. Kutlu, J. Meinl, A. Leuteritz, H. Brünig, S. Wießner, G. Heinrich, Up-scaling of melt-spun LDH/HDPE nanocomposites, Macromol Mater Eng. 299 (2014) 825–833. https://doi.org/10.1002/mame.201300212.

[48] M. Scatto, M. Sisani, Active polymer nanocomposites: Application in thermoplastic polymers, AIP Conf. Proc. 1779 (2016) 040014. https://doi.org/10.1063/1.4965505.

[49] U. Constantino, M. Nocchetti, M. Sisani, R. Vivani, Recent progress in the synthesis and application of organically modified hydrotalcites, Zeithschrift fur Kristollographie 224 (2009) 273-281. https://doi.org/10.1524/zkri.2009.1153.

[50] E. Tarani, I. Arvanitidis, D. Christofilos, D.N. Bikiaris, K. Chrissafis, G. Vourlias, Calculation of the degree of crystallinity of HDPE/GNPs nanocomposites by using various experimental techniques: a comparative study, J Mater Sci. 58 (2023) 1621–1639. https://doi.org/10.1007/s10853-022-08125-4.

[51] A. Kilic, K. Jones, E. Shim, B. Pourdeyhimi, Surface crystallinity of meltspun isotactic polypropylene filaments, Macromol Res. 24 (2016) 25–30. https://doi.org/10.1007/s13233-016-4011-y.

[52] S. Sinha Ray, M. Okamoto, Polymer/layered silicate nanocomposites: A review from preparation to processing, Progress in Polymer Science. 28 (2003) 1539–1641. https://doi.org/10.1016/j.progpolymsci.2003.08.002.

[53] F.R. Costa, U. Wagenknecht, D. Jehnichen, M.A. Goad, G. Heinrich, Nanocomposites based on polyethylene and Mg-Al layered double hydroxide. Part II. Rheological characterization, Polymer (Guildf). 47 (2006) 1649–1660. https://doi.org/10.1016/j.polymer.2005.12.011.

[54] N. Chandran, C. Sarathchandran, S. Thomas, Rheology of polymer-clay nanocomposites, in: Rheology of Polymer Blends and Nanocomposites: Theory, Modelling and Applications, Elsevier, 2019: pp. 97–122. https://doi.org/10.1016/B978-0-12-816957-5.00006-9.

[55] G. Galgali, C. Ramesh, A. Lele, Rheological study on the kinetics of hybrid formation in polypropylene nanocomposites, Macromolecules. 34 (2001) 852–858. https://doi.org/10.1021/ma000565f.

[56] J. Li, C. Zhou, G. Wang, D. Zhao, Study on rheological behavior of polypropylene/clay nanocomposites, J Appl Polym Sci. 89 (2003) 3609–3617. https://doi.org/10.1002/app.12643.

[57] M. El Achaby, F.E. Arrakhiz, S. Vaudreuil, A. El Kacem Qaiss, M. Bousmina, O. Fassi-Fehri, Mechanical, thermal, and rheological properties of graphene-based polypropylene nanocomposites prepared by melt mixing, Polym Compos. 33 (2012) 733–744. https://doi.org/10.1002/pc.22198.

[58] F.R. Costa, M. Abdel-Goad, U. Wagenknecht, G. Heinrich, Nanocomposites based on polyethylene and Mg-Al layered double hydroxide. I. Synthesis and characterization, Polymer. 46 (2005) 4447–4453. https://doi.org/10.1016/j.polymer.2005.02.027.

[59] M. Ardanuy, J.I. Velasco, M. Antunes, M.A. Rodriguez-Perez, J.A. De Saja, Structure and properties of Polypropylene/Hydrotalcite nanocomposites, Polym Compos. 31 (2010) 870–878. https://doi.org/10.1002/pc.20869.

[60] Q. Zhou, V. Verney, S. Commereuc, I.J. Chin, F. Leroux, Strong interfacial attrition developed by oleate/layered double hydroxide nanoplatelets dispersed into poly(butylene succinate), J Colloid Interface Sci. 349 (2010) 127–133. https://doi.org/10.1016/j.jcis.2010.05.015.

[61] N. Mao, C.H. Zhou, D.S. Tong, W.H. Yu, C.X. Cynthia Lin, Exfoliation of layered double hydroxide solids into functional nanosheets, Appl Clay Sci. 144 (2017) 60–78. https://doi.org/10.1016/j.clay.2017.04.021.

[62] D. Tabuani, S. Ceccia, G. Camino, Polypropylene nanocomposites, study of the influence of the nanofiller nature on morphology and material properties, Macromol Symp. 301 (2011) 114–127. https://doi.org/10.1002/masy.201150315.

[63] Y. Zheng, Y. Chen, Preparation of polypropylene/Mg-Al layered double hydroxides nanocomposites through wet pan-milling: formation of a second-staging structure in LDHs intercalates, RSC Adv. 7 (2017) 1520–1530. https://doi.org/10.1039/c6ra26050k.

[64] Q. Yuan, S. Awate, R.D.K. Misra, Nonisothermal crystallization behavior of polypropylene-clay nanocomposites, Eur Polym J. 42 (2006) 1994–2003. https://doi.org/10.1016/j.eurpolymj.2006.03.012.

[65] L. Du, B. Qu, Structural characterization and thermal oxidation properties of LLDPE/MgAl-LDH nanocomposites, J Mater Chem. 16 (2006) 1549–1554. https://doi.org/10.1039/b514319e.

[66] L. Fambri, I. Dabrowska, A. Pegoretti, R. Ceccato, Melt spinning and drawing of polyethylene nanocomposite fibers with organically modified hydrotalcite, J Appl Polym Sci. 131 (2014). https://doi.org/10.1002/app.40277.

[67] F.P. La Mantia, M.C. Mistretta, R. Scaffaro, L. Botta, M. Ceraulo, Processing and characterization of highly oriented fibres of biodegradable nanocomposites, Compos B Eng. 78 (2015) 1–7. https://doi.org/10.1016/j.compositesb.2015.03.054.

[68] T. Yaoita, T. Isaki, Y. Masubuchi, H. Watanabe, G. Ianniruberto, G. Marrucci, Primitive chain network simulation of elongational flows of entangled linear chains: Stretch/orientation-induced reduction of monomeric friction, Macromolecules. 45 (2012) 2773–2782. https://doi.org/10.1021/ma202525v.

[69] E. Nilsson, H. Oxfall, W. Wandelt, R. Rychwalski, B. Hagström, Melt spinning of conductive textile fibers with hybridized graphite nanoplatelets and carbon black filler, J Appl Polym Sci. 130 (2013) 2579–2587. https://doi.org/10.1002/app.39480.

[70] V. Pasanovic-Zujo, R.K. Gupta, S.N. Bhattacharya, Effect of vinyl acetate content and silicate loading on EVA nanocomposites under shear and extensional flow, Rheol Acta. 43 (2004) 99–108. https://doi.org/10.1007/s00397-003-0324-9.

[71] M. Okamoto, P.H. Nam, P. Maiti, T. Kotaka, N. Hasegawa, A. Usuki, A House of Cards Structure in Polypropylene/Clay Nanocomposites under Elongational Flow, Nano Lett. 1 (2001) 295–298. https://doi.org/10.1021/nl0100163.

[72] B. Xu, J. Leisen, H.W. Beckham, R. Abu-Zurayk, E. Harkin-Jones, T. McNally, Evolution of clay morphology in polypropylene/montmorillonite nanocomposites upon equibiaxial stretching: A solid-state NMR and TEM approach, Macromolecules. 42 (2009) 8959–8968. https://doi.org/10.1021/ma901754m.

Supplementary information

Elongational flow-induced microstructure evolutions in polypropylene/layered double hydroxides nanocomposites

Chiara Gnoffo[1], Rossella Arrigo[1,2,*], Michele Sisani[3], Alberto Frache[1,2]

[1] Dipartimento di Scienza Applicata e Tecnologia, Politecnico di Torino, Viale Teresa Michel 5, 15121, Alessandria, Italy

[2] Local INSTM unit

[3] Prolabin & Tefarm S.r.l., Via Dell'Acciaio, 9 06134, Perugia, Italy

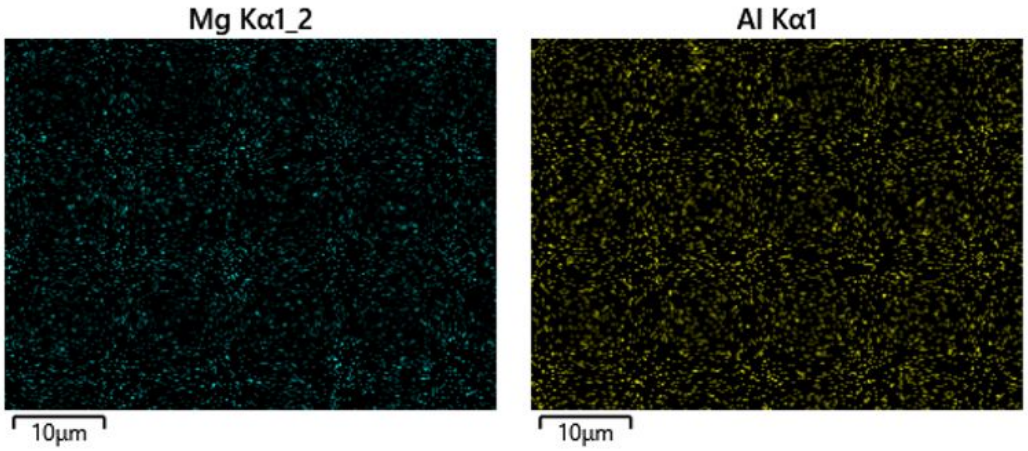

Figure S1. EDX analysis on extruded nanocomposite containing 10 wt % o-LDHs

	Tensile strength [MPa]
PP	4.9
5 wt % s-LDHs	26.0
10 wt % s-LDHs	28.0
5 wt % o-LDHs	29.3
10 wt % o-LDHs	28.9

Table S1. Tensile strength values for isotropic samples